Design and Forming of Chemical Nanomaterials and Their Utilization in Energy Storage and Conversion

Zhanhong Guo[1,a,*], Yadong Liu[2,b], Luyao Li[2,c]

[1]Institute of Chemistry and Chemical Engineering, HFUT (Hefei University of Technology), Xuancheng, Anhui, China
[2]Department of Materials Science and Engineering, HFUT (Hefei University of Technology), Xuancheng, Anhui, China
[a]19339180626@163.com, [b]17333241169@163.com, [c]13781623667@163.com
*Corresponding author

Abstract: With the gradual depletion of non-renewable energy sources such as fossil fuels such as coal, oil, and natural gas, as well as the intensification of environmental problems such as water during industrialization, the search for new energy sources is currently a research hotspot. However, due to the poor conductivity of traditional metal oxides and their significant volume expansion during charging and discharging, their application in energy storage is greatly limited. The main focus of this article was on the design, fabrication, and application of chemical nanomaterials in energy storage and conversion. Based on the physical plating and chemical dealloying process, S/NPCu materials with high quality and stability were prepared. The morphology and composition of the samples were analyzed using SEM (Scanning Electron Microscope), TEM (Transmission Electron Microscope), XRD (X-ray Diffraction), etc. Using filtered CuKα, X-ray diffraction was measured on an X-ray diffractometer. In the electrode system, measurements were made using a rotary disc electrode using linear sweep voltammetry and cyclic voltammetry. Even when the charging and discharging rate reached $4Ag^{-1}$, MnO_2 could still reach $1300mAhg^{-1}$, indicating that it still had good stability during the charging and discharging process. Therefore, by designing the electrode structure reasonably, it is possible to achieve rapid and stable energy storage of nanomaterials with extremely low conductivity.

1. Introduction

The energy issue is a major challenge that humanity would face in the next 50 to 100 years. Traditional mineral fuels such as coal, oil, and natural gas urgently need to find a new renewable energy source to replace traditional mineral energy due to their non-renewability, low energy conversion rate, and environmental pollution caused by utilization. New energy conversion and storage technologies have also emerged. However, due to limitations in material properties, this technology cannot achieve large-scale applications, such as in electric vehicles, energy storage, etc., and cannot simultaneously meet the fast charging and discharging requirements under high energy

density, long cycle performance, and high current density. The performance of such devices mainly depends on the dimensions, morphology, structure, conductivity, and interface properties of the materials. Therefore, the development of new energy storage conversion materials is crucial for the development of energy storage and converter devices.

This article first presents the design, fabrication, and research background and significance of chemical nanomaterials in energy storage and conversion, followed by the preparation of nano porous copper/manganese dioxide composite electrodes. Using physical plating and chemical dealloying process, S/NPCu materials with high quality and stability are prepared. At the same time, the electrochemical performance of the nano porous copper/manganese dioxide electrode is characterized, and finally, the specific performance of the performance surface energy is analyzed.

2. Related Work

Due to the excellent physical, chemical, and biological properties of nanomaterials, they have become important research objects in areas such as optoelectronics, storage, and catalysis. Zhou Wei used Prussian blue compounds such as iron cyanide/graphene oxide as precursors and prepared iron oxide/graphene composite materials by high-temperature cracking method [1]. Lu S introduced the development process of gold wet synthesis technology, with a focus on the core technology of gold liquid phase preparation. On this basis, he introduced some gold nanocrystals with special crystal forms and different phase states [2]. Liyanage T explored the progress of nanomaterials in sensor fabrication technology, and explored the shortcomings of current nanomaterials and their applications in sensitive materials [3]. Zhao H introduced how to control the shape of one-dimensional, two-dimensional, and three-dimensional amorphous nanomaterials in the wet chemical synthesis process, in order to create clear morphologies [4]. Sebastian V reviewed the research progress in the preparation of anisotropic and polygonal nanostructures using microfluidic methods in recent years, with a focus on developing feasible methods for regulating the structure and chemical composition of nanomaterials [5]. However, their research is limited in the application of nanomaterial energy storage and conversion, and cannot achieve perfect energy density.

With the rapid development of portable electronic devices, finding electrode materials with high specific capacity is currently a research hotspot. However, the vast majority of carbon materials have high crystallinity and highly oriented arrangement, which limits the directional infiltration of lithium ions and reduces their electrochemical performance. Transition metal oxides represented by iron oxide, cobalt oxide, nickel oxide, copper oxide, manganese oxide, etc., are an ideal negative electrode material for high specific capacity lithium-ion batteries. However, its poor conductivity, susceptibility to particle aggregation and volume expansion during lithium storage, and other issues limit its practical application.

3. Methods

3.1 Preparation of Nanoporous Copper/Manganese Dioxide Composite Electrode

The negative electrode material of lithium-ion batteries is a key factor determining their performance. At present, there are two main types of negative electrode materials for lithium-ion batteries: carbon based materials and non-carbon based materials. Metal oxides have broad application prospects in the field of lithium-ion batteries due to their low cost, abundant sources, environmental friendliness, and non-toxicity [6-7]. However, during the charging and discharging process, iron oxide particles may agglomerate and collapse, seriously affecting their capacitance performance. Therefore, improving the cycling stability of materials while maintaining high specific capacity is a key scientific issue that urgently needs to be addressed.

The preparation of manganese oxides with high surface area and active sites is an important way to achieve the application of manganese oxide materials, which is beneficial for the research and application of manganese oxides in supercapacitors and catalytic materials. In addition, adding other metal materials with excellent conductivity to manganese oxide can effectively improve its conductivity and reactivity, thereby enhancing its capacitance performance. Nanomaterials have many advantages that cannot be compared to other materials. Constructing composite nanomaterials with multiple morphological compositions at the nanoscale can better utilize the synergistic effects and electron transfer capabilities between materials.

By utilizing block copolymer assembly technology, covalent connections between two or more different types of macromolecules can be achieved [8]. Through the connectivity of molecular chains, controllable phase separation can be achieved. This process can be carried out in both single block copolymers and various block copolymers [9]. In the latter method, block copolymers serve as templates for pores, that is, by removing block polymers, they are made to have a pore structure; on the other hand, it is also a polymer material with a porous structure, which can generate porous polymers during the reaction process and introduce them into the polymer framework [10]. Porous polymers have the dual advantages of both porous and polymer materials, as well as high specific surface area, adjustable pore size, and ease of processing. In recent years, they have received widespread attention. Ultimately, the multifunctionality and controllable structure of polymer materials can be achieved through diverse synthesis pathways [11-12].

Conventional powder electrocatalysts require adhesive coating on the surface of the collector, which inevitably leads to the separation of the active material from the collector, thereby reducing their catalytic activity. By constructing electrode materials with self-supporting structures, it is expected to fundamentally solve this problem and improve the stability of catalytic materials [13]. On this basis, by regulating the crystal plane structure of the catalyst, the proportion of low valent metals on its high index crystal plane is increased, providing more catalytic active sites and improving its catalytic performance. Carbon materials, transition metal oxides, conductive polymers, etc., are currently the most commonly used materials for supercapacitors [14]. The main function of the diaphragm is to block the migration of active materials, avoid short circuits caused by conductivity between electrodes, and place higher requirements on the insulation performance of the diaphragm material, with pores not exceeding the minimum particle size. The main function of electrolytes is to provide ions to capacitors and ensure the balance of their internal charges.

This article adopts a physical plating+chemical dealloying process to prepare S/NPCu materials with high quality and stability. Before plating the copper film, the copper foil is thoroughly washed and dried with acetone and deionized water. Using magnetron sputtering method, $Cu_{30}Mn_{70}$ alloy thin film is deposited on cleaned copper foil [15]. Under the condition of a power of 200W and a sputtering time of 20 minutes, magnetron sputtering technology is adopted. The thickness of the deposited alloy film is 800 nanometers. At room temperature, 10 ml of HCl is used for nitrogen deoxygenation for 30 minutes, allowing the obtained alloy film to undergo 5 hours of alloying at room temperature. To prevent oxygen from entering the solution during dealloying, it is necessary to seal the opening of the reaction vessel with a sealing film. After dealloying, the sample is washed multiple times with deoxidized and deionized water, and dried to obtain S/NPCu. S/NPCu is placed in a mixture of 5ml $KMnO_4$ and 10ml KOH, completely submerged, and then placed in a closed hydrazine hydrate environment for 30 minutes to obtain $S/NPCu/MnO_2$. Before magnetron sputtering, the dealloyed S/NPCu is weighed and the mass of NPCu is calculated. Based on the mass ratio of NPCu to Cu/MnO_2 measured by energy spectrum, the loading amount of MnO_2 is calculated.

3.2 Electrochemical Performance Characterization of Nano Porous Copper/Manganese Dioxide Electrodes

A good electrode material not only needs to have a high electron transfer rate, but also needs to have a stable structure. However, the development of metal (hydrogen) oxides as high-performance electrode materials is limited due to their poor conductivity, slow ion migration rate, and large volume expansion during lithium insertion.

The morphology and composition of the sample are analyzed using SEM, TEM, XRD, etc. Using filtered CuKα, X-ray diffraction is measured on an X-ray diffractometer. Raman spectroscopy is obtained using a 532nm laser on a Raman spectrometer. The prepared electrodes are assembled into the glove box of the 2016 model button battery. Among them, the prepared electrode is a positive electrode, while the lithium plate is a negative electrode. The current voltage curve is measured on the electrochemical workstation, and charge discharge tests are conducted on the test platform, with a voltage range of 0.01-3.0V. Under certain conditions, applying a certain amount of alternating current causes the electrode potential to shift, thereby obtaining the variation of electrode impedance with frequency. By using an equivalent simulation circuit, impedance spectra are fitted and the kinetic parameters of electrode chemical reactions are obtained.

The current density (I_a) and specific capacitance (C_a) of MnO$_2$ in the composite electrode are calculated using the following formulas:

$$I_a = I/m \tag{1}$$

$$C_a = R/m \tag{2}$$

In the formulas, m is the mass of MnO$_2$. The mass ratio of positive and negative electrode reactants is calculated using the following formula:

$$\frac{m}{n} = \frac{C_a \Delta V}{\Delta V_n} \tag{3}$$

In the formula, n is the mass of activated carbon.

The button battery punching machine is used to punch the dried coating to obtain a circular electrode with a diameter of 12 millimeters. To avoid loose and detached coating after drying, a powder tablet press is used to press the plates. The copper foil and electrode plate are weighed separately and placed in a dry sealed bag for later use. 20mg of the prepared nanocomposite material is added to a 250ml beaker and stirred in a dark room for 90 minutes in a newly prepared 100mL solution of 10mg/L methylene blue until absorption reached equilibrium. Then, the beaker is placed 15 centimeters under a xenon lamp and its absorption rate is measured using a UV spectrometer.

3.3 Electrochemical Property Testing

(1) Electrocatalytic hydrogen evolution test

It is stirred in distilled water for 5-6 hours to obtain a uniform slurry. Scrapers are used to evenly coat copper foil, and then the coating is dried in a vacuum oven at 100 °C for 12 hours to remove moisture. After the tubular electric furnace cools naturally at room temperature, the black powder obtained from calcination is taken out, and then sonicated with 1 M dilute hydrochloric acid for 30 minutes. Then, it is poured to allow the black suspension on it to precipitate. Firstly, the black suspension is centrifuged, then washed several times with distilled water and ethanol, and then dried under vacuum at 60 °C for 6 hours to obtain a black solid sample. An electrocatalytic hydrogen production experiment is conducted on a 5 mV s^{-1} three electrode system using 0.5MH$_2$SO$_4$ as the electrolyte. Using a nano porous copper/manganese dioxide electrode as the working electrode, a

surface modified working electrode with a loading capacity of 0.29 mg cm^{-2} is prepared by uniformly applying 5μL of catalyst slurry onto the surface using a micropipette gun and drying at room temperature.

(2) Electrocatalytic oxygen reduction test

Hydrogen oxygen fuel cells are an efficient way of energy utilization, which can convert chemical energy into electrical energy. This energy conversion process only involves water and does not produce pollution. It can effectively reduce carbon dioxide emissions and has a high conversion efficiency. Hydrogen oxygen fuel cells oxidize hydrogen on the cathode, producing electrons that are then transmitted through an external circuit to the cathode, promoting the reduction of oxygen. Electrocatalytic oxygen reduction is a reaction that involves multiple electron transfers, with two main reaction pathways: one is the four electron reduction pathway, where oxygen is reduced to water; one is a double electron reduction reaction, where oxygen is reduced to hydrogen peroxide. The four electron reduction reaction can be further divided into two categories: direct four electron reduction and stepwise four electron reduction. The four electron reduction reaction has a high reduction current and low toxicity, but the reduction products produced by the two electron reduction reaction not only greatly reduce the stability of the catalyst, but also cause irreversible damage to the entire device.

In three electrode systems, measurements are made using a rotary electrode using linear sweep voltammetry and cyclic voltammetry. Using a 0.1 MKOH solution as the electrolyte and a cyclic voltammetry scan rate of 50 mV s^{-1}, a linear scan of 10 mV s^{-1} is performed, and the rotational speed of the rotating disk electrode is controlled at 400-2500 rpm. Using a nano porous copper/manganese dioxide electrode as the working electrode, a pre prepared catalyst of 10μL is uniformly applied to the surface using a micropipette, dried at room temperature, and a surface modified working electrode with a loading capacity of 0.2 mg cm^{-2} is prepared.

4. Results and Discussion

4.1 Electrochemical Performance Characterization Results of Nano Porous Copper/Manganese Dioxide Electrode

The comparison of rate performance between S/NP Cu/MnO$_2$ composite bulk electrode and nano manganese dioxide under changes in current density is shown in Figure 1. Although the conductivity of oxides is poor, the seamless integration of S/NP Cu/MnO$_2$ composite electrodes can effectively improve their rate performance. For S/NP Cu/MnO$_2$, when the current density is 9Ag^{-1}, the discharge capacity of MnO$_2$ is 1300mAhg^{-1}; when the current density is 15Ag^{-1}, the discharge capacity of MnO$_2$ is 998mAhg^{-1}; when the current density is 140Ag^{-1}, it is 650mAhg^{-1}. Even when the charging and discharging rate reaches 4Ag^{-1}, MnO$_2$ can still reach 1300 mAhg^{-1}, indicating that it still has good stability during the charging and discharging process.

The comparison of specific capacities of porous membrane S/NPCu/MnO$_2$ composite materials with thicknesses of 0.8μm and 1.2μm at different current densities is shown in Figure 2. Although low dimensional nanomaterials can shorten the distance of ion transport, while conductive materials can accelerate the transport of electrons, the contact resistance between their internal current collector/electrode materials and low dimensional nano structural elements, as well as the weak interface interaction between conductive materials (such as nanocarbon) and active materials, result in limited improvement in their specific capacity and rate performance. At a current density of 0.02mAcm^{-2}, the specific capacities of porous membrane S/NPCu/MnO$_2$ composites with thicknesses of 0.8μm and 1.2μm are 0.14mAcm^{-2} and 0.22 mAcm^{-2}, respectively. In fact, the capacitance of the electrode mainly comes from the MnO$_2$ generated by the reduction of KMnO4 by hydrazine hydrate.
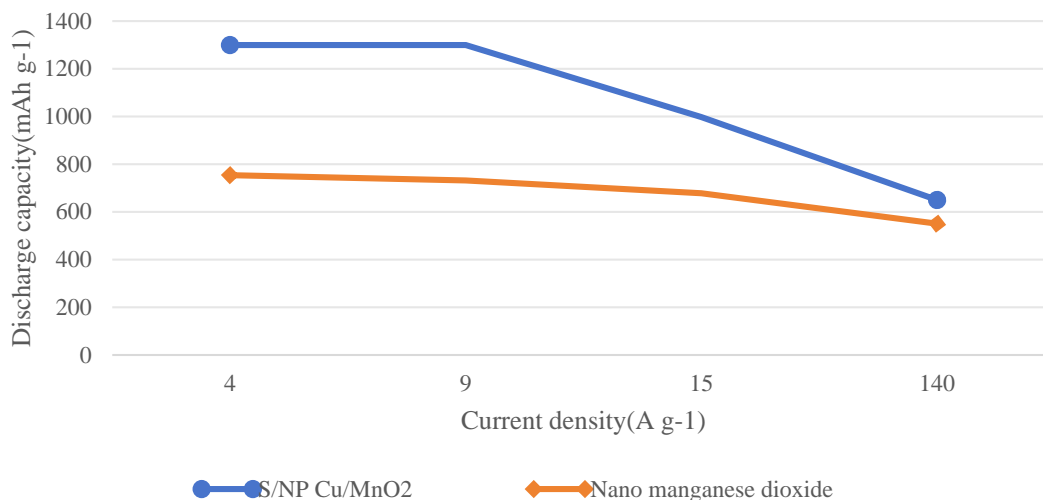
Figure 1: Comparison of rate performance between S/NP Cu/MnO$_2$ composite bulk electrode and nano manganese dioxide under changes in current density
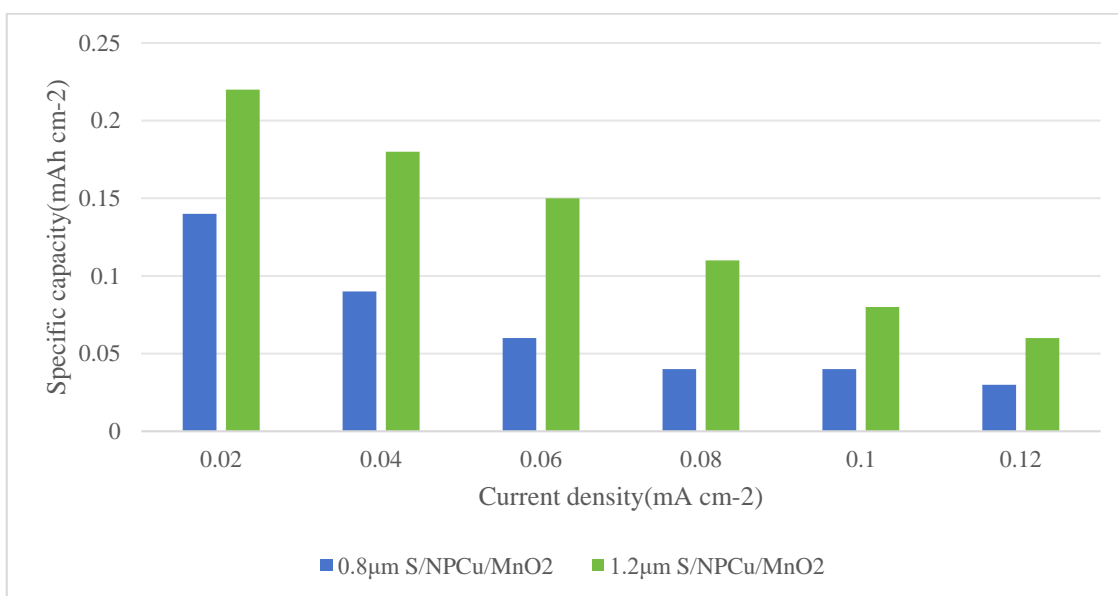

Figure 2: Comparison of specific capacities of porous membrane S/NPCu/MnO$_2$ composite materials with thicknesses of 0.8μm and 1.2μm at different current densities

The comparison of the curves of NPAu/Ni(OH)$_2$ and CFP/Ni(OH)$_2$ electrodes at a scanning speed of 500mVs^{-1} is shown in Figure 3. Compared with CFP/Ni(OH)$_2$, NPAu/Ni(OH)$_2$ has a higher current response. The reason for this is that the vertically grown Ni(OH)$_2$ single crystal and the Au/Ni(OH)$_2$ coherent interface formed by epitaxial growth are conducive to electron and ion migration within Ni(OH)$_2$ and at the Au/Ni(OH)$_2$ interface.
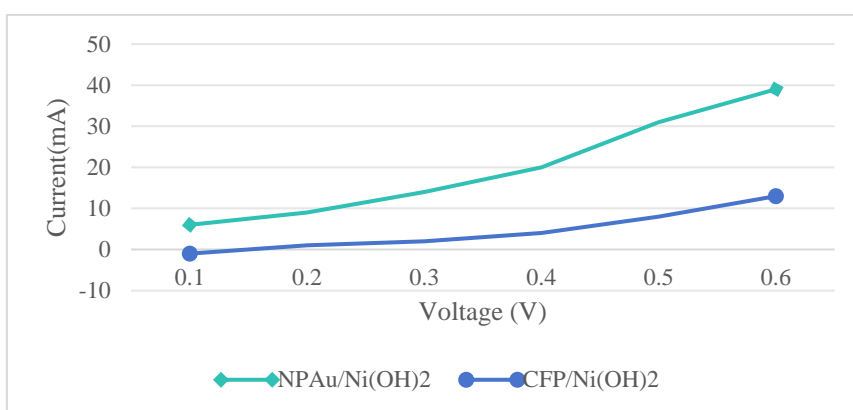
Figure 3: Comparison of curves of NPAu/Ni(OH)$_2$ and CFP/Ni(OH)$_2$ electrodes at a scanning speed of 500mVs^{-1}

4.2 Electrochemical Test Results

The charging and discharging experimental data of S/NPCu/SnO$_2$ electrode under a voltage of 0.005-3.0V are shown in Table 1. When the current density is 0.09, 0.4, 0.7, 1.3, 4, 7, 13Ag^{-1}, the specific capacity of SnO$_2$ is 1105,898,790,719,596,460 and 333mAg^{-1}, indicating that the S/NPCu/SnO$_2$ electrode has better charge discharge performance.

Table 1: Experimental data on charging and discharging of S/NPCu/SnO2 electrodes at voltages ranging from 0.005 to 3.0V

Current density (A g^{-1})	Specific capacity (mAh g^{-1})
0.09	1105
0.4	898
0.7	790
1.3	719
4	596
7	460
13	333

The charge comparison between the battery type and lithium-ion capacitive type of S/NPCu/MnO$_2$ composite electrode is shown in Table 2. Due to the lack of strong interaction interface between Cu/MnO$_2$ and the dispersion effect of S/NPCu, manganese dioxide nanoparticles are directly supported on copper sheets, resulting in disordered stacking on their surfaces and high contact resistance with copper, leading to a decrease in their specific capacitance and rate performance. When the scanning speed is below 10mV s^{-1}, the stored charge in the battery type memory exceeds 70%. The S/NPCu/MnO$_2$ composite electrode combines both battery and capacitor energy storage characteristics, and has extremely high rate performance.

Table 2: Charge comparison between battery type and lithium-ion capacitive type of S/NPCu/MnO2 composite electrode

Scanning speed (mVs^{-1})	Battery type(%)	Capacitive type(%)
5	75%	65%
10	62%	67%
15	59%	70%
20	60%	69%
25	45%	72%

5. Conclusions

With the advancement of technology in fields such as electronics, electric vehicles, and aerospace, the demand for energy is also increasing. This article fully leveraged the advantages of nanomaterials and focused on various transition metal compounds as research objects. Through the study of energy storage and conversion of different types of transition metal compounds (such as electrolysis of water for hydrogen production, fuel cell oxygen reduction, etc.), the impact of different types of transition metal compounds on energy storage and conversion was deeply analyzed, and their applications in energy storage and conversion were explored. By utilizing the pore structure of NPCu and the stable interface of Cu/MnO_2, the volume expansion of MnO_2 during charging and discharging processes and the stable recombination with conductive components are ensured to ensure the stability of its energy storage performance. On this basis, by designing the electrode structure reasonably, energy storage materials with high magnification and high stability are obtained.

References

[1] Zhou Wei, Wu Zhong, Li Tinghu, et al. Preparation and electrochemical properties of iron oxide graphene nanomaterials. Shandong Chemical, 2020, 49 (13): 1-3.

[2] Lu S, Liang J, Long H, et al. Crystal phase control of gold nanomaterials by wet-chemical synthesis. Accounts of Chemical Research, 2020, 53(10): 2106-2118.

[3] Liyanage T, Qamar A Z, Slaughter G. Application of nanomaterials for chemical and biological sensors: A review. IEEE Sensors Journal, 2020, 21(11): 12407-12425.

[4] Zhao H, Li F, Wang S, et al. Wet chemical synthesis of amorphous nanomaterials with well-defined morphologies. Accounts of Materials Research, 2021, 2(9): 804-815.

[5] Sebastian V. Toward continuous production of high-quality nanomaterials using microfluidics: Nanoengineering the shape, structure and chemical composition. Nanoscale, 2022, 14(12): 4411-4447.

[6] Lang R, Du X, Huang Y, et al. Single-atom catalysts based on the metal–oxide interaction. Chemical reviews, 2020, 120(21): 11986-12043.

[7] Li Y, Zhang Y, Qian K, et al. Metal–support interactions in metal/oxide catalysts and oxide–metal interactions in oxide/metal inverse catalysts. ACS Catalysis, 2022, 12(2): 1268-1287.

[8] Karayianni M, Pispas S. Block copolymer solution self-assembly: Recent advances, emerging trends, and applications. Journal of Polymer Science, 2021, 59(17): 1874-1898.

[9] Shin J J, Kim E J, Ku K H, et al. 100th anniversary of macromolecular science viewpoint: Block copolymer particles: Tuning shape, interfaces, and morphology. ACS Macro Letters, 2020, 9(3): 306-317.

[10] Taylor D, Dalgarno S J, Xu Z, et al. Conjugated porous polymers: incredibly versatile materials with far-reaching applications. Chemical Society Reviews, 2020, 49(12): 3981-4042.

[11] Wang Q, Unno M, Liu H. Organic–inorganic hybrid near-infrared emitting porous polymer for detection and photodegradation of antibiotics. ACS Sustainable Chemistry & Engineering, 2022, 10(22): 7309-7320.

[12] Mansour F R, Arrua R D, Desire C T, et al. Non-ionic surface active agents as additives toward a universal porogen system for porous polymer monoliths. Analytical Chemistry, 2021, 93(5): 2802-2810.

[13] Heard D M, Lennox A J J. Electrode materials in modern organic electrochemistry. Angewandte Chemie International Edition, 2020, 59(43): 18866-18884.

[14] Zhang Y, Jiang J, An Y, et al. Sodium-ion capacitors: materials, mechanism, and challenges. ChemSusChem, 2020, 13(10): 2522-2539.

[15] Liang J, Liu Q, Li T, et al. Magnetron sputtering enabled sustainable synthesis of nanomaterials for energy electrocatalysis. Green Chemistry, 2021, 23(8): 2834-2867.